

A Computing Objective Tensor Fields

Objective tensor fields are reference frame-independent, which is a necessary condition that the properties they describe are fundamental aspects of the flow rather than artifacts of a particular observational standpoint. We have identified many objective quantities in the literature and will briefly review the ones we utilize in our experiments, highlighting their significance in the study of material boundaries in 2D unsteady flow fields.

A fundamental tool in our analysis is the *flow map*, which describes the evolution of fluid particle positions over time. The flow map

$$\begin{aligned}\Phi_{t_0}^t : M &\rightarrow M, \\ x_0 &\mapsto \Phi_{t_0}^t(x_0),\end{aligned}\tag{27}$$

maps the initial position x_0 of a particle at time t_0 to its position at a later time t , along the particle's trajectory (path line) from time t_0 to time t . The flow map is defined for all possible positions in the fluid domain, and therefore encapsulates the trajectories of all particles through the fluid domain. This mapping is essential for understanding the displacement and deformation of fluid elements and is integral to the computation of other derived quantities.

The flow map not only encodes the trajectories of particles, but also serves as foundational tool to measure how differential structures are advected by the flow. Particularly, the gradient of the flow map, denoted as $D\Phi$, is of interest in the definition of objective scalar fields. By interpreting the flow map as a diffeomorphism that maps all points of the manifold of the fluid domain onto itself after a finite time t , we can offer a geometric interpretation of $D\Phi$. Specifically, $D\Phi$ is also called the *pushforward* in differential geometry. The pushforward represents the linear mapping of vectors between the tangent spaces of a particle moving from position x_0 to position $\Phi_{t_0}^t(x_0)$.

A vector \mathbf{v} at the tangent space at x_0 is mapped to its image at time t by the pushforward $D\Phi(\mathbf{v})$. The pushforward $D\Phi(\mathbf{v})$, describes the mapping of all possible vectors from the tangent space at x_0 to the tangent space at x_t . Analyzing this mapping is crucial as it reveals how different vectors — and by extension, fluid elements — rotate and scale under the transformation $D\Phi(\mathbf{v})$, thereby indicating how the fluid itself rotates and deforms. Since $D\Phi(\mathbf{v})$ is a linear mapping, we can easily utilize mathematical tools to quantify the rotational and deforming characteristics of the flow.

It is important to note that neither the flow map by itself, nor its gradient are invariant to reference frame transformations. However, they capture the essence of the fluid dynamics that are objective.

Right Cauchy-Green Deformation Tensor

We can use the pushforward of the flow map to define the *right Cauchy-Green deformation tensor* as

$$C = (D\Phi)^T (D\Phi),\tag{28}$$

where $(D\Phi)^T$ represents the transpose of the pushforward $D\Phi$. In any choice of coordinate system, this tensor can be represented as a symmetric positive-definite matrix which measures the change in distances and angles between material elements. By further examining C , we can derive scalar quantities that describe the flow's

behavior, such as strain rates and rotation rates, in an objective manner that is independent of the observer's frame of reference. To extract material boundaries of the flow field, we are naturally interested in the amount of stretching that happens under the mapping of the flow map and the associated pushforward. This stretching can be quantified by computing the direction of maximal stretching as the first eigenvector of the symmetric tensor C . The first eigenvalue, which quantifies the amount of stretching at each point, is an objective scalar field which we use to find separating boundaries in the flow.

Finite-Time Lyapunov Exponents

The finite-time Lyapunov exponent (FTLE) quantifies the rate of separation of infinitesimally close particle trajectories over a finite time interval, offering insights into the dynamic behavior of fluid flows. The FTLE is fundamentally linked to the right Cauchy-Green deformation tensor C , through the computation of the maximum eigenvalue of C over a time interval from t_0 to t at a point x_0 , and can be expressed as

$$\sigma_{t_0}^t(x_0) = \frac{1}{|t - t_0|} \log \sqrt{\lambda_{\max}(x_0)},\tag{29}$$

where $\lambda_{\max}(x_0)$ is the maximum eigenvalue of the tensor C at the point x_0 . This expression highlights how the FTLE measures the exponential rate of divergence of particle trajectories, with higher values indicating regions of significant material stretching or folding.

When computing $\lambda_{\max}(x_0)$ forward in time ($t > t_0$), high FTLE values indicate repelling LCS, while when computing $\lambda_{\max}(x_0)$ backward in time ($t < t_0$) high FTLE values indicate attracting LCS.

B Additional Results

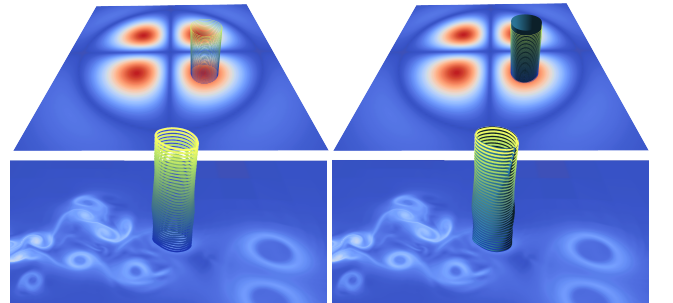


Figure 8: Interactive Iso-Contour Components: (left) Iso-contour component preview computed interactively and visualized in the local reference frame. (right) Iso-contours overlaid on resulting iso-surface.

On the left of Fig. 8 we show results from our novel interactive iso-contour preview visualization. On the right of Fig. 8 we show the corresponding iso-surfaces that are computed in the local reference frame. We note that the interactive preview visualization only works in situations where a suitable reference frame is found. In contrast without the computation of the reference frame (i.e., in the original reference frame) an interactive preview would only work for fluid flow structures that largely stay in place or happen to be steady. Since this is typically not the case - our novel preview visualization method is only feasible when considering a local reference frame.

In Fig. 9 we compare our method (iso-surface extraction in the local reference frame) with the iso-surface extraction in the original frame when the time domain is under-sampled (i.e., fluid structures move at a speed where surface extraction methods fail in the original reference frame). In Fig. 9 we show a cropped region of the Boussinesq dataset and compute iso-surfaces with VTK from a deliberately under-sampled dataset. We under-sample the dataset in the time domain to test our reference frame based approach. From top to bottom we show the original resolution ($\text{dim } t = 32$) and successively reduce the number of samples in the time domain by a factor of two. The surfaces are color-coded using Normal Deviation (ND), where lower ND values indicate smoother surfaces. The conventional approach introduces significant geometric and topological artifacts due to temporal under-sampling. A good local reference frame can still combat the under-sampling when reconstructing a fluid flow structure that moves with a speed where the conventional approach fails.

In Fig. 10 we use our method to extract and analyze material boundary candidates in the local reference frame of the synthetic Bickley jet function. The Bickley jet is a mathematical model used to describe and analyze geophysical fluid dynamics. It represents a simplified way to understand the behavior of jet streams or oceanic currents. The model consists of a series of sinusoidal waves superimposed on a mean flow, which together mimic the meandering nature of real jet streams or currents. This idealized configuration allows scientists to study the stability, wave interactions, and energy dispersion within these geophysical phenomena in a more controlled and analytical framework.

We compare the material boundary candidates extracted from several state of the art vortex region methods. Our method allows us to compare the results of multiple methods in the local reference frame of the vortex structures. Fig. 10 shows the iso-surfaces of the

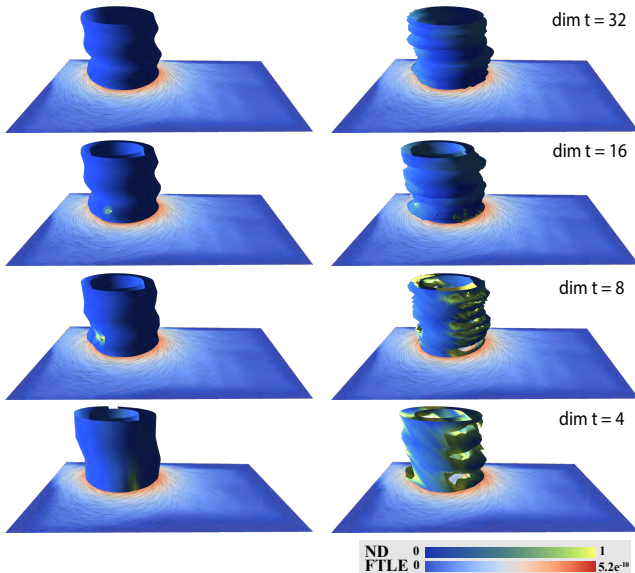


Figure 9: Temporal under-sampling: Comparing surface extraction in the original reference frame (right) with surface extraction in the local reference frame (left) in the case of temporal under-sampling.

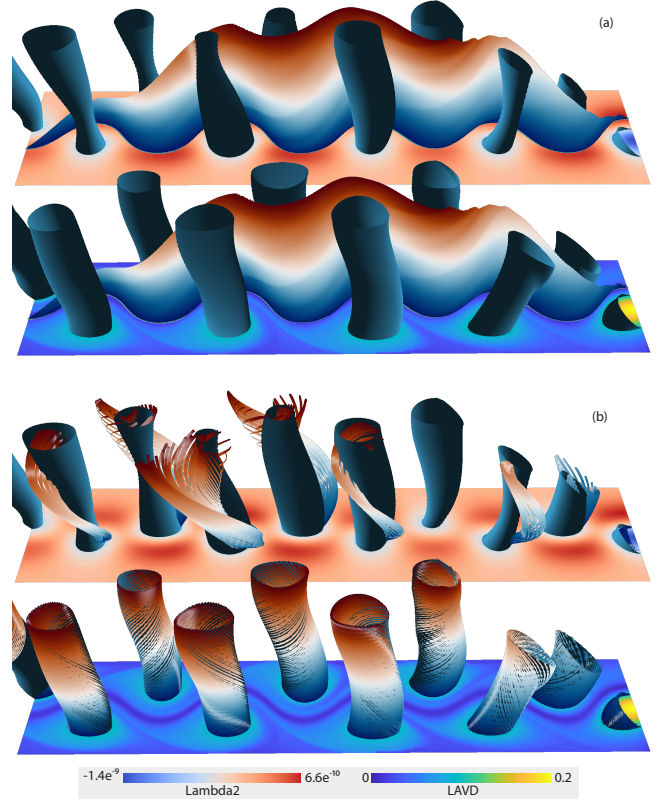


Figure 10: Comparing vortex criteria in local reference frames. Iso-surfaces of Lambda2 criterion and LAVD. (a) the model of the jet stream visualized as timeline seeded on the zero iso-contour of vorticity at time zero, advected over time. Top of (a) Lambda2 iso-surfaces, bottom of (a) LAVD iso-surfaces. (b) The same iso-surfaces as in (a) visualized together with path lines seeded at time zero exactly at the iso-contours of the surfaces. Top of (b) Lambda2 iso-surfaces do not contain the path lines seeded on their iso-contours. Bottom of (b) LAVD iso-surfaces perfectly agree with the path lines advected from their iso-contours.

Lambda2 criterion and LAVD. Fig. 10 (a) shows the iso-surfaces (blue) together with the model of the jet stream visualized as a timeline seeded on the zero iso-contour of vorticity deviation at time zero and advected over time (time axis is vertical - color coding blue to red). Fig. 10 (a) shows that Lambda2 iso-surfaces as well as LAVD iso-surfaces are situated next to the modeled jet stream that flows between them. In Fig. 10 (b), the same iso-surfaces as in (a) are shown. This time they are visualized together with path lines seeded at time zero at the iso-contours of the surfaces. The top of Fig. 10 (b) shows that Lambda2 iso-surfaces do not contain the path lines seeded at their iso-contours. The bottom of Fig. 10 (b) shows that LAVD iso-surfaces perfectly agree with the path lines starting at their iso-contours at time zero.

This tells us that in ideally modeled situations LAVD is better suited for material boundary extraction. Our method makes it possible to analyze Lagrangian structures in the local reference frame with high accuracy surface extraction. In this case the visualization shows perfect agreement of LAVD material boundaries and path line trajectories.